Miniaturization of Laser Doppler Vibrometers

Subjects: Instruments & Instrumentation

Contributor: Yanlu Li , Emiel Dieussaert , Roel Baets , Zhizhi Yang

Laser Doppler vibrometry (LDV) is a non-contact vibration measurement technique based on the Doppler effect of the reflected laser beam. Thanks to its feature of high resolution and flexibility, LDV has been used in many different fields today. The miniaturization of the LDV systems is one important development direction for the current LDV systems that can enable many new applications.

laser Doppler vibrometry miniaturization photonic integrated circuit

1. PIC-Based LDV

Laser Doppler vibrometry (LDV) can be realized on various photonic integrated circuit (PIC) platforms which are available today. The most popular PIC platforms include silicon-on-insulator (SOI) [1][2], GaAs [3][4], InP [5][6], lithium niobate [7], silica-based planar lightwave circuit (PLC) [8], silicon-nitride [9][10], and polymers [11]. In these platforms, light is not propagating in free space but is guided in very compact single-mode waveguides. A typical dimension of the cross-section of an SOI waveguide is 450 nm × 220 nm. These small waveguides can be bent to a very small radius without significant optical loss [12]. As a result, the footprint of the PIC can be greatly reduced. This bend radius is ultimately determined by the refractive index contrast (RIC) between the waveguide material and the cladding material. A higher RIC value means better confinement of the guided optical mode in the waveguide and a smaller acceptable bend radius. For example, the RIC of an optical fiber is relatively small (e.g., 0.36% [13]). Therefore, the bend radius of most optical fiber cannot be smaller than millimeters. On the contrary, the RIC of a deeply etched waveguide in the SOI platform is 3.48/1.45, which is high enough to reduce the bend radius to around 2 microns in the SOI platform. Among these aforementioned platforms, the SOI platform shows the highest RIC at 1550 nm.

Another important figure of merit of these platforms is the optical loss in PIC, which mainly includes the loss in a single-mode waveguide and the loss between a single-mode fiber and the optical interconnect components of the PIC, i.e., grating couplers and butt couplers. The waveguide loss is mainly caused by optical scattering at the imperfect boundaries of the waveguide core and cladding. Therefore, reducing the electric field at the waveguide walls can suppress optical waveguide loss. Generally speaking, PIC platforms with lower RIC values have larger mode diameters and, therefore, lower normalized field strengths. As a result of the reduced normalized field strength at the waveguide boundaries, they have lower waveguide losses. However, as mentioned above, the minimum bend radius of the waveguide is larger than that with a higher RIC due to the lower RIC. To reduce optical loss while keeping a small bend radius, one can also improve the waveguide's boundary quality during the fabrication process [14] or use special waveguide designs such as shallowly etched optical waveguides to reduce the area of scattering boundaries [15]. It is known that silica platforms have very low waveguide losses (<0.1 dB/cm) thanks to their low RIC values, while the ridge waveguides (deeply etched) in SOI with higher RIC values have higher waveguide losses. Note that when the optical power in the waveguide is much higher (e.g., when the optical power in an SOI ridge waveguide is larger than 10 mW), and the nonlinear optical loss caused by, e.g., two-photon absorption, will become significant and should be considered [16]. Dielectric platforms (SiN, silica) suffer much less from this limitation than semiconductor platforms (SOI, InP, and GaAs).

Butt couplers and grating couplers are usually used to couple light from single-mode fibers to the PIC. They are also used as the optical antennas in the LDV PIC to transmit and receive signals to and from the target [17]. Butt couplers couple light from the waveguide to free space at the edge of the PIC. If the mode size of the waveguide is much smaller than the mode size of a single-mode optical fiber (which is the case for most of the PIC platforms), butt couplers need a spot-size converter on the end of the waveguide to ensure a good coupling efficiency [18]. Grating couplers couple light from the waveguide out of the plane to free space using the diffraction effect of a grating [19]. The coupling efficiency of butt coupling is generally better than that of a grating coupler. However, grating couplers are very popular in PIC because they do not have a location limitation: they can be positioned anywhere on the chip. Furthermore, grating couplers also enable wafer-level testing that cannot be realized by butt couplers.

Based on the waveguide structures, various photonic components can be realized on one chip. These include the necessary components needed by an LDV interferometer: optical splitter, combiner, directional couplers, and 90° hybrid. In addition, LDV also requires some active optical components, such as laser source, phase modulators, PDs, and OFSs (heterodyne). In conventional LDVs, light reflected to the laser source will reduce the stability of the laser signal. Therefore, optical isolators are also required. Currently, none of the PIC platforms have all the necessary components for LDV and, therefore, dominates over the other platforms. For example, SOI does not have high-performance monolithically integrated laser sources due to the indirect bandgap of crystalline silicon. Therefore, many different integration methods have been applied to implement these components. For example, Germanium PDs are integrated on the SOI platform using monolithic integration [20], while III-V material-based laser diodes can be implemented on the SOI platform using a heterogeneous integration method [21] or a hybrid integration method (e.g., using the micro-optical bench [22]).

2. Self-Mixing LDV

The self-mixing LDV uses an interference technique different from the standard LDV. The technique is called laser feedback interferometry (LFI) [23][24] or optical feedback interferometry (OFI) [25]. The self-mixing effect was first reported by King et al. in 1963 [26] and was then used in a laser Doppler velocimetry system by Rudd et al. in 1968 [27]. A typical self-mixing LDV sensor has a simpler configuration compared to the standard LDV described above. It only consists of two major components: a laser diode and a PD that is placed next to the laser and detects its optical power (see **Figure 1**). Some self-mixing designs do not even have the PD and use the laser terminal voltage as the monitoring signal [28], which makes the device smaller than a PIC-based LDV system. During measurement, light from the self-mixing LDV is sent to the target and then reflected back to the laser source by the test target. The feedback light is reinjected to the laser source and introduces a perturbation in the laser's cavity, which leads to a change in the measurable parameters of the laser, e.g., the optical power and the laser terminal voltage.

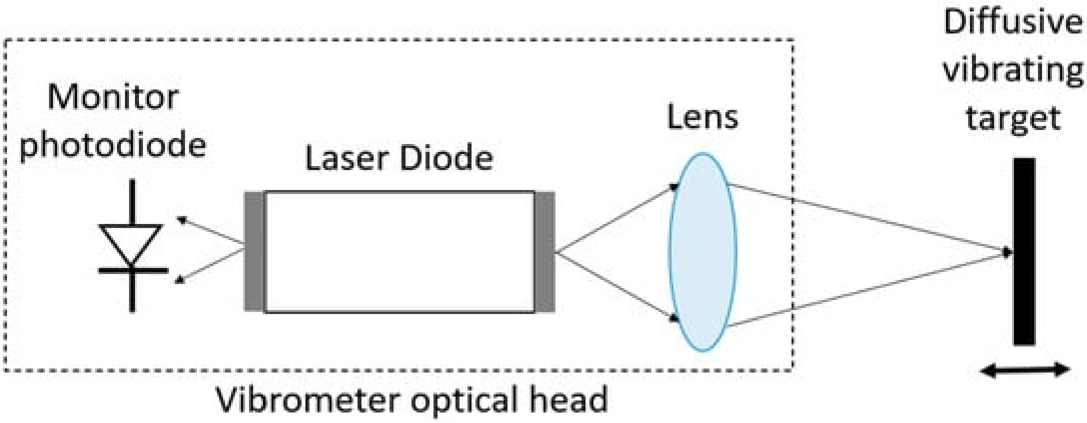

Figure 1. A typical configuration of a self-mixing LDV.

However, the monitoring signals of self-mixing LDVs are much more complicated than those of standard LDVs. One apparent phenomenon of a self-mixing LDV system is the direction-dependent saw-tooth shape in the monitoring signal [28].The shape of the saw-tooth changes as a function of the feedback power [29], which is normally described by the injection parameter (or feedback parameter) *C*. It is calculated as follows:

$C = \kappa \frac{\tau_{ext}}{\tau_{laser}} \sqrt{1+\alpha^2}$where the following

$$\kappa = \varepsilon(1-R_2)\sqrt{\frac{R}{R_2}}$$

is the coupling strength coefficient of external reflection, R is the reflectance of light at the laser facet, R2 is the reflectance of the target, *ε* is the loss of reflected light caused by, e.g., mode mismatch, α is the linewidth enhancement factor of the laser, τext is the round-trip time of flight in the external cavity, and τlaser is the round-trip time of flight in the laser cavity. To be more specific, there are five different performance regimes in self-mixing interferometry [23][30] (see **Figure 2**) that correspond to different monitoring shapes. For self-mixing LDVs, the researchers only discuss the phenomenon in regimes I–III. They are the weak optical feedback regime I (*C* ≤ 1), moderate optical feedback regime II (*C* > 1), and strong optical feedback regime III (*C* >> 1). When the reflection is even stronger, the system will be working the regime IV or V, where the self-mixing technique will not be applicable. To be in the self-mixing regime, the feedback power should be reduced by more than 35 dB.

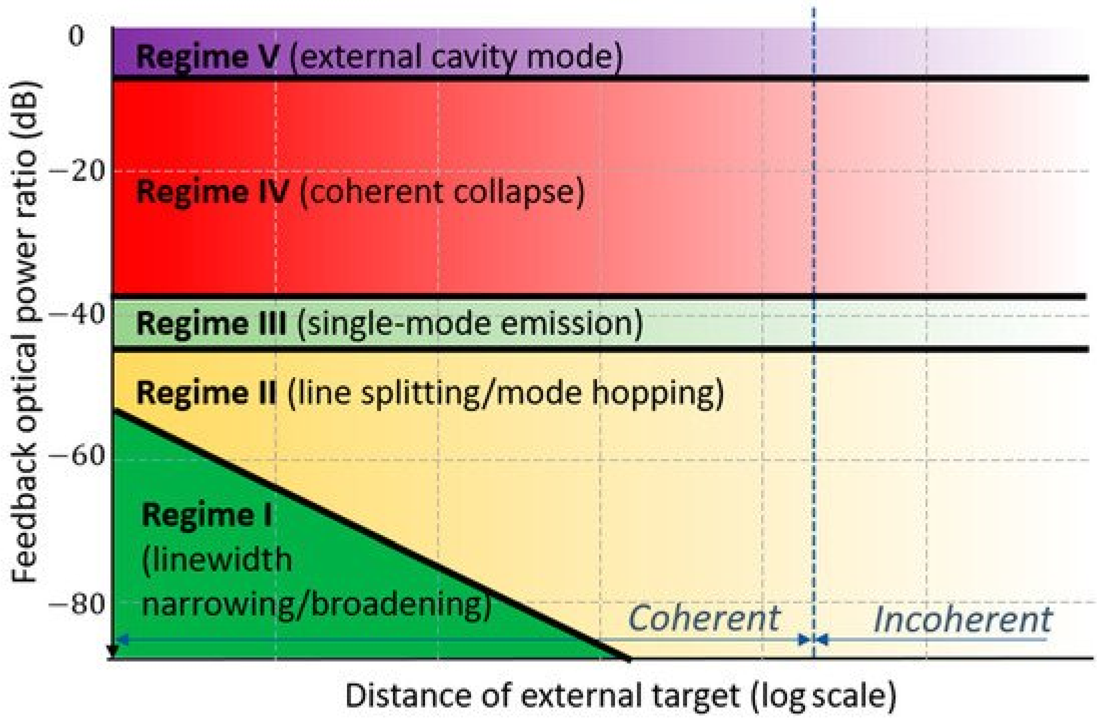

Figure 2. The five different regimes of laser feedback. Adapted from Refs. [30][31].

These complex phenomena are usually explained by the three-mirror cavity model [32][33] or the Lang–Kobayashi model [34]. In the three-mirror cavity model, the reflection target is considered an extra mirror of the laser cavity. The change of the optical power in the laser is a mutual effect of the three-mirror cavity. In the Lang–Kobayashi model, the electric field in the laser cavity is considered a slowly varying electric field. The amplitude and phase of this field are assumed to be disturbed by external feedback. The information of the external cavity (e.g., length) is described in the coupled term of the external feedback. Both models provide the same results. A detailed description of these theories can be found in [23].

Due to the complex relationship between reflection and output signal, various approximation methods are developed for different purposes. If self-mixing is used to measure the displacement of a target and the resolution is larger than λ/2, one can use a fringe counting method to count the number of fringes in the monitoring signal. The direction of the movement can be determined by the shape of the signals when the measurement is operated at the $C > 1$ regime. If the vibration is smaller than λ/2, it is also possible to retrieve the vibration signal of the target by using the linear region of the response curve of the self-mixing LDV. However, it is required to place the vibration center in the center position of the monitor signal. This can be realized by tuning the wavelength of the laser. Another method to measure the vibration information is based on retrieving the frequency shifts of the photocurrent signals. This can be realized by either using spectrum analyzers or frequency demodulators. Spectrum analyzers are only used to measure slowly varying vibrations. Frequency demodulators can measure vibrations at higher frequencies, but the optical reflection usually needs to be kept low (regime I) to ensure good measurement accuracy. The detailed frequency demodulation method of a self-mixing device can be found in [35].

However, these methods have a limited dynamic range. To increase the dynamic range, one can retrieve the displacement signal based on the solution to the equations derived from the aforementioned three-mirror theories [36] or based on the minimization of a cost function [37]. However, these methods are very difficult for real-time reconstruction.

One method to improve the recovery dynamic range is to use a two-mode (e.g., two orthogonal modes) operation for the laser source. In this design, one laser mode is used to measure the target's vibration, and the other mode is used for generating a quadrature signal (I and Q) [38][39]. However, this is not used in a laser diode, because generating two orthogonal modes with the desired properties (e.g., stable frequency separation) is difficult [31]. Therefore, this technique has not been established in miniaturized self-mixing LDVs.

A closed-loop vibrometry based on analog feedback has been reported in [40]. In this research, the feedback loop uses the interferometric photocurrent signal as the error, which is converted to a modulation in the driving current of the laser diode. Since the wavelength is proportional to the driving current, the wavelength can be changed accordingly to compensate for the interferometric phase change caused by the movement of the target. The target displacement is retrieved from the modulated driving current signal. This vibrometer shows a noise equivalent velocity of 100 pm/sqrt (Hz) and a 180 µm peak-to-peak maximum measurable vibration. Magnani et al. demonstrated a digital closed-loop feedback [24] self-mixing vibrometer. However, this method requires the knowledge of the absolute distance of the target from the sensor to measure the displacement/velocity. Therefore, other methods [41] should be used to retrieve the target distance, which renders the complete system more complicated.

Self-mixing can be combined with a frequency shifter, e.g., an acousto-optical modulator (AOM), to perform a heterodyne self-mixing effect [42] (**Figure 3**). As mentioned in the section, using the heterodyning method in self-mixing can improve the SNR of the LDV signal and suppress nonlinear harmonics. Additionally, using AOM can also realize multi-beam vibration detections with a single laser diode. This multipoint detection is realized by converting the vibration signals in the spatial domain to the frequency domain with the help of the multiple diffraction beams of AOM [43].

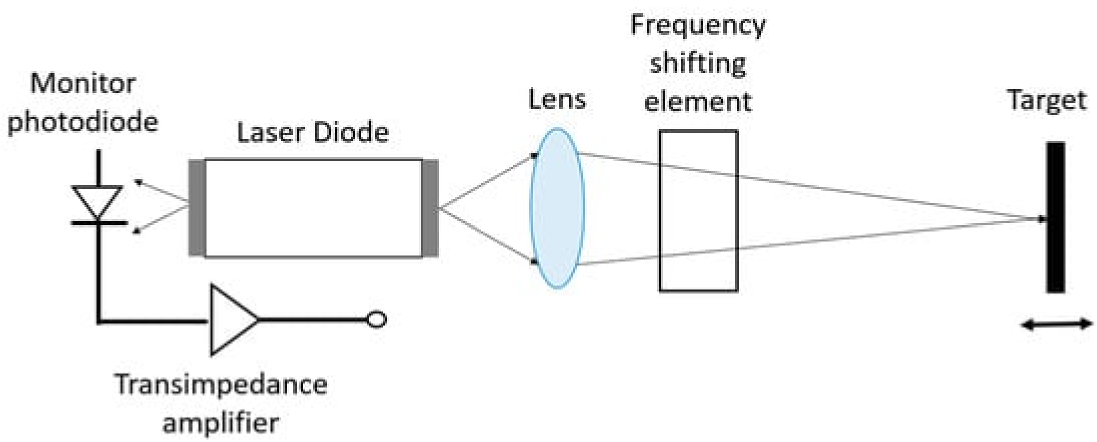

Figure 3. A schematic configuration of a self-mixing heterodyne LDV.

3. Micromachined Free-Space Interferometer of LDV

The optical interferometer used for LDV can also be realized with miniaturized free-space micro-opto-electromechanical systems (optical MEMS) [44]. The micromachined Michelson interferometer has been demonstrated in a silicon-on-insulator (SOI) platform for various applications such as a Fourier transform spectrometer [45][46]. In reference [47][48], micromachined MIs are used for displacement measurement, which is close to the function of LDV. This design has a footprint that is smaller than 1 cm^2 and it has a probe with 4 mm length, 550 µm width, and 400 µm depth. The light is sent into the interferometer using an optical fiber placed on a fiber groove carved in the chip, while the combined signal is sent to another fiber via which the light signal finally reaches the photodetector. The displacement resolution is around 0.04 nm, which is limited by electronic noise. However, this design cannot be used to determine the direction of the movement. MEMS-based MZIs are also demonstrated [49]. However, this design was not designed to detect the vibrations of external targets. Therefore, no real LDV has been demonstrated in optical MEMS.

To realize a proper LDV that can discriminate the movement directions, either the 90-degree optical hybrid or the frequency shifter is needed. To the best knowledge of the authors, these components are still missing in optical MEMS. Therefore, no LDV has been demonstrated in the MEMS up until now. To realize a MEMS-based LDV, the following challenges should be addressed: Firstly, light diffraction is very strong in the MEMS system since the beam diameter is usually very small. Therefore, MEMS components for collimating or focusing light beams should be developed. Deep etching depth is also needed to ensure a good optical throughput for expanded optical beams. Secondly, more advanced optical components, such as a 90° hybrid for homodyne LDV, need to be developed in the optical MEMS system. Thirdly, light is sent into and out of the interferometer system via optical fibers [44], which limits the compactness of the entire system. Therefore, methods for integrating laser sources, optical isolators, photodetectors, and optical frequency shifters will be developed in the optical MEMS system to ensure the compactness of the entire system.

The implementation of a multi-beam LDV is a further step of MEMS-based LDV after the realization of a single-beam LDV. More optical components such as 1 × N optical splitters are needed in this case, which leads to more challenges. The 1 × N optical splitter solution may be realized with cascaded beam splitters or a group of beam splitters facing in different directions. Another solution is to combine the optical MEMS with an AOM, in which the multiple diffraction beams of the AOM can be used as a multi-beam LDV (such as [43]). Generally speaking, there are still many challenges to conquer in implementing a multibeam MEMS-based LDV.

References

1. Jian Wang; Yun Long; On-chip silicon photonic signaling and processing: a review. *Science Bulletin* **2018**, *63*, 1267-1310, 10.1016/j.scib.2018.05.038.

2. Po Dong; Young-Kai Chen; Guang-Hua Duan; David T. Neilson; Silicon photonic devices and integrated circuits. *Nanophotonics* **2014**, *3*, 215-228, 10.1515/nanoph-2013-0023.
3. Jianwei Wang; Alberto Santamato; Pisu Jiang; Damien Bonneau; Erman Engin; Joshua W. Silverstone; Matthias Lermer; Johannes Beetz; Martin Kamp; Sven Höfling; et al.Michael G. TannerChandra M. NatarajanRobert H. HadfieldSander N. DorenbosVal ZwillerJeremy L. O'BrienMark G. Thompson Gallium arsenide (GaAs) quantum photonic waveguide circuits. *Optics Communications* **2014**, *327*, 49-55, 10.1016/j.optcom.2014.02.040.
4. Christof P. Dietrich; Andrea Fiore; Mark G. Thompson; Martin Kamp; Sven Höfling; GaAs integrated quantum photonics: Towards compact and multi-functional quantum photonic integrated circuits (Laser Photonics Rev. 10(6)/2016). *Laser & Photonics Reviews* **2016**, *10*, 857-857, 10.1002/lpor.201670065.
5. Meint Smit; Xaveer Leijtens; Huub Ambrosius; Erwin Bente; Jos Van Der Tol; Barry Smalbrugge; Tjibbe De Vries; Erik-Jan Geluk; Jeroen Bolk; Rene Van Veldhoven; et al.Luc AugustinPeter ThijsDomenico D'AgostinoHadi RabbaniKatarzyna LawniczukStanisław StopińskiSaeed TahviliAntonio CorradiEmil KleijnDzmitry DzibrouManuela FelicettiElton BitinckaValentina MoskalenkoJing ZhaoRui SantosGiovanni GilardiWeiming YaoKevin WilliamsPatty StabilePiet KuindersmaJosselin PelloSrivathsa BhatYuqing JiaoDominik HeissGunther RoelkensMike WalePaul FirthFrancisco SoaresNorbert GroteMartin SchellHelene DebregeasMohand AchoucheJean-Louis GentnerArjen BakkerTwan KorthorstDominic GallagherAndrew DabbsAndrea Ivano MelloniFrancesco MorichettiDaniele MelatiAdrian WonforRichard PentyRonald BroekeBob MuskDave Robbins An introduction to InP-based generic integration technology. *Semiconductor Science and Technology* **2014**, *29*, 083001, 10.1088/0268-1242/29/8/083001.
6. Meint Smit; Kevin Williams; Jos Van Der Tol; Past, present, and future of InP-based photonic integration. *APL Photonics* **2019**, *4*, 050901, 10.1063/1.5087862.
7. A. Rubiyanto; H. Herrmann; R. Ricken; F. Tian; W. Sohler; Integrated Optical Heterodyne Interferometer in Lithium Niobate. *Journal of Nonlinear Optical Physics & Materials* **2001**, *10*, 163-168, 10.1142/s0218863501000516.
8. Hiroshi Takahashi; High performance planar lightwave circuit devices for large capacity transmission. *Optics Express* **2011**, *19*, B173-B180, 10.1364/oe.19.00b173.
9. Daniel J. Blumenthal; Rene Heideman; Douwe Geuzebroek; Arne Leinse; Chris Roeloffzen; Silicon Nitride in Silicon Photonics. *Proceedings of the IEEE* **2018**, *106*, 2209-2231, 10.1109/jproc.2018.2861576.
10. Abdul Rahim; Eva Ryckeboer; Ananth Z. Subramanian; Stephane Clemmen; Bart Kuyken; Ashim Dhakal; Ali Raza; Artur Hermans; Muhammad Muneeb; Soren Dhoore; et al.Yanlu LiUtsav DavePeter BienstmanNicolas Le ThomasGunther RoelkensDries Van ThourhoutPhilippe

HelinSimone SeveriXavier RottenbergRoel Baets Expanding the Silicon Photonics Portfolio With Silicon Nitride Photonic Integrated Circuits. *Journal of Lightwave Technology* **2016**, *35*, 639-649, 10.1109/jlt.2016.2617624.

11. Roger Dangel; Antonio La Porta; Daniel Jubin; Folkert Horst; Norbert Meier; Marc Seifried; Bert J. Offrein; Polymer Waveguides Enabling Scalable Low-Loss Adiabatic Optical Coupling for Silicon Photonics. *IEEE Journal of Selected Topics in Quantum Electronics* **2018**, *24*, 1-11, 10.1109/jstqe.2018.2812603.
12. Shankar Kumar Selvaraja, Purnima Sethi. Review on Optical Waveguides; Kok Yeow You, Eds.; IntechOpen : Vienna, Austria, 2018; pp. 384 .
13. Corning, S.M.F. 28e Optical Fiber Product Information; Corning: New York, NY, USA, 2005.
14. Slevaraja, S. Wafer-Scale Fabrication Technology for Silicon Photonic Integrated Circuits. Ph.D. Thesis, Ghent University, Ghent, Belgium, 2011.
15. W. Bogaerts; S. K. Selvaraja; Compact Single-Mode Silicon Hybrid Rib/Strip Waveguide With Adiabatic Bends. *IEEE Photonics Journal* **2011**, *3*, 422-432, 10.1109/jphot.2011.2142931.
16. Eric Dulkeith; Yurii A Vlasov; Xiaogang Chen; Nicolae C Panoiu; Richard M Osgood; Self-phase-modulation in submicron silicon-on-insulator photonic wires.. *Optics Express* **2006**, *14*, 5524–5534.
17. Yanlu Li; Roel Baets; Homodyne laser Doppler vibrometer on silicon-on-insulator with integrated 90 degree optical hybrids. *Optics Express* **2013**, *21*, 13342-13350, 10.1364/oe.21.013342.
18. José Manuel Luque-González; Robert Halir; Juan Gonzalo Wangüemert-Pérez; José De-Oliva-Rubio; Jens H. Schmid; Pavel Cheben; Íñigo Molina-Fernández; Alejandro Ortega-Moñux; An Ultracompact GRIN-Lens-Based Spot Size Converter using Subwavelength Grating Metamaterials. *Laser & Photonics Reviews* **2019**, *13*, 1900172, 10.1002/lpor.201900172.
19. Dirk Taillaert; Frederik Van Laere; Melanie Ayre; Wim Bogaerts; Dries Van Thourhout; Peter Bienstman; Roel Baets; Grating Couplers for Coupling between Optical Fibers and Nanophotonic Waveguides. *Japanese Journal of Applied Physics* **2006**, *45*, 6071-6077, 10.1143/jjap.45.6071.
20. Steven J. Koester; Jeremy D. Schaub; Gabriel Dehlinger; Jack O. Chu; Germanium-on-SOI Infrared Detectors for Integrated Photonic Applications. *IEEE Journal of Selected Topics in Quantum Electronics* **2006**, *12*, 1489-1502, 10.1109/jstqe.2006.883160.
21. Di Liang; John E. Bowers; Recent Progress in Heterogeneous III-V-on-Silicon Photonic Integration. *Light: Advanced Manufacturing* **2021**, *2*, 59-25, 10.37188/lam.2021.005.
22. Matthieu Duperron; Lee Carroll; Marc Rensing; Sean Collins; Yan Zhao; Yanlu Li; Roel Baets; Peter O'Brien; Hybrid integration of laser source on silicon photonic integrated circuit for low-cost

interferometry medical device. *Imaging, Manipulation, and Analysis of Biomolecules, Cells, and Tissues XII* **2017**, *10109*, 1010915-1010915-17, 10.1117/12.2250921.

23. Thomas Taimre; Milan Nikolić; Karl Bertling; Yah Leng Lim; Thierry Bosch; Aleksandar D. Rakić; Laser feedback interferometry: a tutorial on the self-mixing effect for coherent sensing. *Advances in Optics and Photonics* **2015**, *7*, 570-631, 10.1364/aop.7.000570.
24. Jiyang Li; Haisha Niu; Yan Xiong Niu; Laser feedback interferometry and applications: a review. *Optical Engineering* **2017**, *56*, 050901-050901, 10.1117/1.oe.56.5.050901.
25. Yu Zhao; Julien Perchoux; Lucie Campagnolo; Thierry Camps; Reza Atashkhooei; Véronique Bardinal; Optical feedback interferometry for microscale-flow sensing study: numerical simulation and experimental validation. *Optics Express* **2016**, *24*, 23849, 10.1364/oe.24.023849.
26. King, P.; Steward, G. Metrology with an optical maser. New Sci. 1963, 17, 180.
27. M J Rudd; A laser Doppler velocimeter employing the laser as a mixer-oscillator. *Journal of Physics E: Scientific Instruments* **1968**, *1*, 723-726, 10.1088/0022-3735/1/7/305.
28. Edson T. Shimizu; Directional discrimination in the self-mixing type laser Doppler velocimeter. *Applied Optics* **1987**, *26*, 4541-4544, 10.1364/ao.26.004541.
29. M. H. Koelink; M. Slot; F. F. M. De Mul; J. Greve; R. Graaff; A. C. M. Dassel; J. G. Aarnoudse; Laser Doppler velocimeter based on the self-mixing effect in a fiber-coupled semiconductor laser: theory. *Applied Optics* **1992**, *31*, 3401-3408, 10.1364/ao.31.003401.
30. R. Tkach; A. Chraplyvy; Regimes of feedback effects in 1.5-µm distributed feedback lasers. *Journal of Lightwave Technology* **1986**, *4*, 1655-1661, 10.1109/jlt.1986.1074666.
31. S. Donati; Developing self-mixing interferometry for instrumentation and measurements. *Laser & Photonics Reviews* **2011**, *6*, 393-417, 10.1002/lpor.201100002.
32. Peter J. De Groot; Gregg M. Gallatin; Steven H. Macomber; Ranging and velocimetry signal generation in a backscatter-modulated laser diode. *Applied Optics* **1988**, *27*, 4475-4480, 10.1364/ao.27.004475.
33. W. M. Wang; W. J. O. Boyle; K. T. V. Grattan; A. W. Palmer; Self-mixing interference in a diode laser: experimental observations and theoretical analysis. *Applied Optics* **1993**, *32*, 1551-1558, 10.1364/ao.32.001551.
34. R. Lang; K. Kobayashi; External optical feedback effects on semiconductor injection laser properties. *IEEE Journal of Quantum Electronics* **1980**, *16*, 347-355, 10.1109/jqe.1980.1070479.
35. Yufeng Tao; Ming Wang; Wei Xia; Carrier-separating demodulation of phase shifting self-mixing interferometry. *Optics & Laser Technology* **2017**, *89*, 75-85, 10.1016/j.optlastec.2016.08.013.

36. S. Donati; G. Giuliani; S. Merlo; Laser diode feedback interferometer for measurement of displacements without ambiguity. *IEEE Journal of Quantum Electronics* **1995**, *31*, 113-119, 10.1109/3.341714.

37. G. Plantier; C. Bes; T. Bosch; Behavioral model of a self-mixing laser diode sensor. *IEEE Journal of Quantum Electronics* **2005**, *41*, 1157-1167, 10.1109/jqe.2005.853364.

38. T. Giallorenzi; J. Bucaro; A. Dandridge; G. Sigel; J. Cole; S. Rashleigh; R. Priest; Optical fiber sensor technology. *IEEE Journal of Quantum Electronics* **1982**, *18*, 626-665, 10.1109/jqe.1982.1071566.

39. S. Donati; Laser interferometry by induced modulation of cavity field. *Journal of Applied Physics* **1978**, *49*, 495-497, 10.1063/1.324672.

40. Guido Giuliani; Simone Bozzi-Pietra; Silvano Donati; Self-mixing laser diode vibrometer. *Measurement Science and Technology* **2002**, *14*, 24-32, 10.1088/0957-0233/14/1/304.

41. Jiyang Li; Haisha Niu; Laser feedback interferometry and applications: a review. *Optical Engineering* **2017**, *56*, 050901-050901, 10.1117/1.oe.56.5.050901.

42. Zang, D.; Millerd, J. Heterodyned Self-Mixing Laser Diode Vibrometer. U.S. Patent 5,838,439, 17 November 1998.

43. Y. Fu; M. Guo; P. B. Phua; Spatially encoded multibeam laser Doppler vibrometry using a single photodetector. *Optics Letters* **2010**, *35*, 1356-1358, 10.1364/ol.35.001356.

44. Yasser M. Sabry; Diaa Khalil; Tarik Bourouina; Monolithic silicon-micromachined free-space optical interferometers onchip. *Laser & Photonics Review* **2014**, *9*, 1-24, 10.1002/lpor.201400069.

45. Kyoungsik Yu; Daesung Lee; Uma Krishnamoorthy; Namkyoo Park; Olav Solgaard; Micromachined Fourier transform spectrometer on silicon optical bench platform. *Sensors and Actuators A: Physical* **2006**, *130-131*, 523-530, 10.1016/j.sna.2005.12.022.

46. B. Saadany; H. Omran; M. Medhat; F. Marty; D. Khalil; T. Bourouina; MEMS tunable Michelson interferometer with robust beam splitting architecture. *2009 IEEE/LEOS International Conference on Optical MEMS and Nanophotonics* **2009**, -, 49-50, 10.1109/omems.2009.5338601.

47. Hichem Nouira; Jean-Pierre Wallerand; Maurine Malak; Anne-Françoise Obaton; José Salgado; Tarik Bourouina; Miniature silicon Michelson interferometer characterization for dimensional metrology. *Sensors and Actuators A: Physical* **2015**, *223*, 141-150, 10.1016/j.sna.2014.12.031.

48. M. Malak; F. Marty; H. Nouira; G. Vailleau; T. Bourouina; All-silicon Michelson instrument on chip: Distance and surface profile measurement and prospects for visible light spectrometry. *Applied Physics Letters* **2013**, *102*, 141102, 10.1063/1.4801778.

49. Haitham Omran; Mostafa Medhat; Bassem Mortada; Bassam Saadany; Diaa Khalil; Fully Integrated Mach-Zhender MEMS Interferometer With Two Complementary Outputs. *IEEE Journal*

of Quantum Electronics **2011**, *48*, 244-251, 10.1109/jqe.2011.2170825.